Neutron-diffraction study of the solid layers at the liquid-solid boundary in ^{4}He films adsorbed on graphite

K. Carneiro
Physics Laboratory I, H.C. Ørsted Institute Universtetsparken 5, DK-2100 Copenhagen Ø, Denmark

L. Passell and W. Thomlinson
Physics Department, Brookhaven National Laboratory, Upton, New York 11973

H. Taub
Physics Department, University of Missouri-Columbia, Columbia, Missouri 65211
(Received 26 November 1980)

A neutron scattering study of the structure of ^{4}He films adsorbed on graphite is reported. Diffraction from helium monolayers at a temperature of 1.2 K shows the formation of an incommensurate, triangular-lattice solid of high density. As the coverage is increased above two layers, the diffraction pattern changes indicating solidification of a second layer. The observed two-layer patterns can be indexed with either a pair of incommensurate, triangular-lattice solid layers of different densities or a close-packed bilayer; the experimental information available is not sufficient to make a more precise identification. A measurement of the height of the first helium layer above the graphite basal plane was also made. This was done by determining the coverage-dependent shift in the position of the graphite (002) diffraction peak (assumed to arise from interference between film and substrate scattering) and fitting it to a simple structural model. Values for the monolayer height above the graphite plane and for the lattice constants of the possible bilayer structures are given.

I. INTRODUCTION

Exfoliated graphites are often used as substrates in superfluid film studies. Films of helium on Grafoil,[1] for example, have been much investigated. One of the major aims of these experiments has been to probe the microscopic structure of the superfluid-solid boundary. Thus far, the first layer of atoms—the layer immediately adjacent to the graphite surface—has been the most completely explored. Heat-capacity[2] and neutron-diffraction[3] measurements show this layer to form a $(\sqrt{3}\times\sqrt{3})R30°$ epitaxial phase and, at higher coverages, a dense triangular-lattice solid phase incommensurate in structure with the underlying graphite. The second layer has not yet been as well characterized. There is, however, evidence of its melting, seen in the form of a relatively broad peak in the heat capacity. This peak, after first making its appearance at coverages slightly exceeding two layers, narrows progressively with increasing coverage indicating that the layer is subjected to increasing lateral and vertical compression.[4] But, beyond the fact that the average density of the two-layer film is less than that of the monolayer, nothing is known of the bilayer structure. Layers subsequent to the second are known to be liquid[5]; there is also evidence of a substrate-induced density gradient extending several interatomic distances into the liquid from the solid layers at the boundary.

In an effort to better define the structure of the boundary (especially the second layer), we have made a systematic study of neutron diffraction from two- and three-layer ^{4}He films adsorbed on Grafoil. We find evidence of diffraction from both the first and second layer of atoms as well as an enhancement of the graphite (002) reflection due to interference between film and substrate scattering. It is our intention to describe these measurements here and discuss their implications concerning layer structure and height above the graphite basal plane.

We should also note that diffraction studies similar in some respects to our own have recently been reported by Lauter, Wiechert, and Feile.[6]

II. EXPERIMENTAL APPARATUS AND METHOD

The sample used was composed of 51.4 g of Grafoil disks. These, after baking in vacuum at 950 °C, were stacked in a cylindrical aluminum cell 4 cm high and 4 cm in diameter with walls 0.05 cm thick in the region traversed by the neutron beam. A thin-walled Cu-Ni capillary provided access to the cell for helium transfer. Temperatures were measured with a calibrated Ge cryoresistor.

The surface area of the Grafoil substrate was deter-

mined from a nitrogen adsorption isotherm. Thereafter, helium coverages in the cell were defined by filling it with gas from a calibrated external volume (at a known pressure) using for pressure measurements an MKS Baratron gauge.

All diffraction scans were made with a fixed neutron wavelength $\lambda = 2.478$ Å using a triple-axis spectrometer with pyrolytic graphite monochromating and analyzing crystals. Higher-order (shorter wavelength) neutrons were removed from the incident beam by passing it through a pyrolytic graphite filter. To improve background discrimination the spectrometer was operated in the three-axis mode with the analyzer set to accept only elastically scattered neutrons.

The sample cell was mounted so that the neutron scattering vector $\vec{Q} \equiv \vec{k}_i - \vec{k}_f$ was parallel to the graphite foil planes. ($\vec{k}_i$ and $\vec{k}_f$ represent, respectively, the wave vectors of the incident and scattered neutrons.) As is usual in such experiments, diffraction from the films was taken to be the difference between scattered intensities with and without helium in the cell. Every scan was repeated a sufficient number of times to ensure adequate statistical accuracy and to make certain that the observed profiles were not subject to drift due to either film annealing or instrumental anomalies.

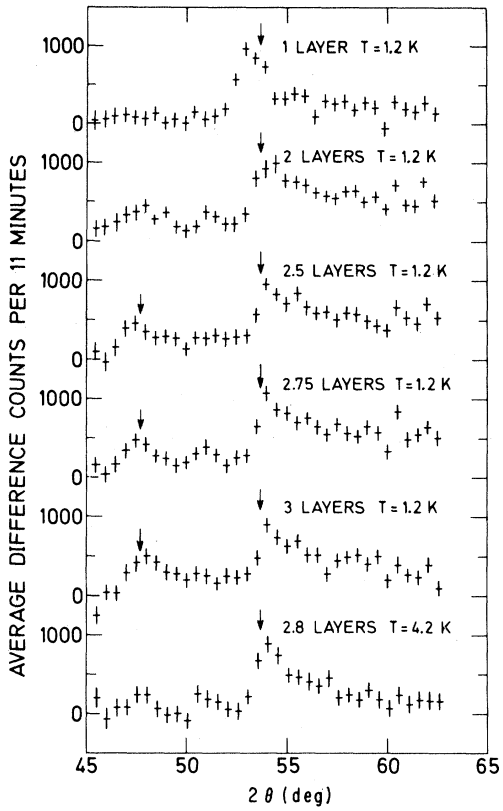

FIG. 1. Coverage dependence of difference-diffraction profiles from ^{4}He films adsorbed on Grafoil. The arrows identify peak positions expected from heat-capacity determinations of the layer densities. Heat-capacity measurements indicate that the second layer is melted at 4.2 K.

III. EXPERIMENTAL RESULTS

A. Diffraction from helium layers

Figure 1 shows a sequence of difference diffraction scans made at a fixed temperature of 1.2 K with helium coverages between one and three layers. Also included is one scan made after heating the three-layer film to 4.2 K (0.2 of the third layer was desorbed during the heating process). To convert from atomic surface density—the quantity measured experimentally—to layers, we assumed the first-layer density to be 0.115 atoms/Å^2, the second to be 0.092 atoms/Å^2, and the third to be 0.056 atoms/Å^2 as given by heat-capacity measurements.[7]

Concentrating for the moment on the first-layer prrofile, we note that it consists of a single peak at a scattering angle $2\theta = 53°$ [$Q = (4\pi/\lambda)\sin\theta = 2.27$ Å^{-1}]. The "sawtooth" shape is characteristic of diffraction from randomly-oriented, two-dimensional arrays. No other peaks were observed. If we assume, as a working hypothesis, that the peak is the lowest-index peak, i.e., the (10) peak, from a triangular lattice (the closest-packed two-dimensional structure), it then follows that the nearest-neighbor distance $a_{NN} = \lambda/(\sqrt{3}\sin\theta)$ and that the film density $\rho = 2/(\sqrt{3}a_{NN}^2)$. Substituting the measured values for λ and θ in the first of these expressions yields $a_{NN} = 3.21$ Å and $\rho = 0.112$ atoms/Å^2. The latter compares well with the value 0.115 atoms/Å^2 obtained from heat-capacity measurements.

Looking at the higher-coverage scans, we note a shift to larger angles in the position of the first-layer peak—indicating compression—and, at two layers, the appearance of a broad, ill-defined structure at $2\theta = 48°$ (probably the scattering from a liquid second layer) which quickly narrows at higher coverages to become a well-defined peak at $2\theta = 47.7°$ ($Q = 2.03$ Å^{-1}).

We begin by interpreting the low-angle peak as originating from an ordered second layer of helium atoms uncorrelated with the first layer. Assuming, as before, that we are observing the (10) peak from a triangular lattice, we obtain values of the nearest-neighbor distance which vary from 3.53 to 3.57 Å (depending on the coverage). The resulting structure, shown in Fig. 2(a), gives second-layer densities from 0.091 to 0.093 atoms/Å^2. Once again, agreement with the layer density obtained from heat-

TABLE I. Plane spacing of the observed reflections (d) and nearest-neighbor distances (a_{NN}) and atomic densities (ρ) in the first three layers of ^{4}He adsorbed on Grafoil assuming two independent layers. All measurements were made at a temperature of 1.2 K except the 2.8-layer scan, which was made at 4.2 K.

Number of layers	First layer			Second layer			Third layer
	d (Å)	a_{NN} (Å)	ρ (Å^{-2})	d (Å)	a_{NN} (Å)	ρ (Å^{-2})	ρ (Å^{-2})
1.0	2.78	3.21	0.112		. . .	. . .	. . .
2.0	2.73	3.15	0.116		. . .	0.091[a]	. . .
2.5	2.72	3.15	0.117	3.09	3.57	0.091	0.028[a]
2.75	2.72	3.15	0.117	3.08	3.55	0.092	0.042[a]
3.0	2.72	3.14	0.117	3.05	3.53	0.093	0.056[a]
2.8	2.73	3.15	0.116			0.091[a]	0.049[a]

[a]Density determined from gas filling.

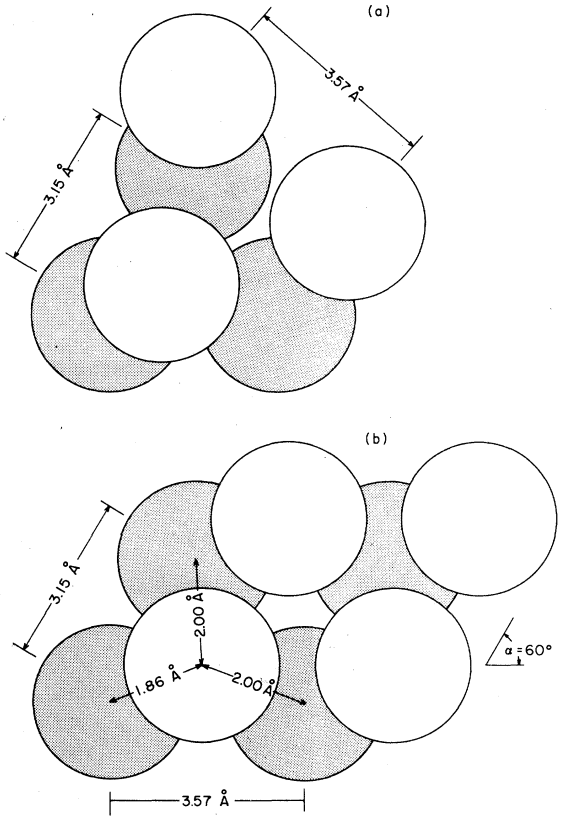

FIG. 2. (a) Projection onto the substrate plane of the proposed independent layer structure. (b) Equivalent projection of the proposed oblique bilayer structure. The shaded circles represent atoms in the first layer, the open circles second-layer atoms. With the positions of the second-layer atoms in the oblique cell as shown, the intensity ratios for the (10), (11), and (01) Bragg reflections are 0.45:0.38:1, respectively, assuming a Debye-Waller factor of unity. Note that in the oblique cell chosen, each second-layer atom is nearly equidistant from three atoms in the first layer.

capacity measurements is excellent.

Further support for an independent layer structure is obtained from the fact that it leads to a correct prediction of the observed intensity ratios. Using Warren's theory of diffraction from random two-dimensional arrays,[8] it is easy to show that the peak intensities from two such layers should be in the ratio $\exp(-2W_2)(\sin\theta_1)^{3/2}/\exp(-2W_1)(\sin\theta_2)^{3/2}$, the W's representing the appropriate Debye-Waller factors for each layer. Although Debye-Waller factors for helium films on graphite have not, as yet, been measured, they can be estimated with sufficient accuracy for our purposes by using the zero-temperature approximation for a two-dimensional Debye solid $2W=\hbar^2Q^2/mk_B\theta_D$ with m being the atomic mass and θ_D, the Debye temperature of the film.[9] Heat-capacity measurements[10] give for the Debye temperatures of films of the suggested densities of the first and second layers the values 58 and 25 K, respectively. Substituting in the above formula leads to a prediction of 0.50 for the intensity ratio I_2/I_1, a value in acceptable agreement with the observed ratios, all of which fall within the range from 0.55 to 0.64.

Table I lists the nearest-neighbor distances and layer densities obtained assuming two independent triangular layers. Where relevant, the densities given are those determined from the positions of diffraction peaks; otherwise, they were inferred from the measured quantity of gas on the substrate surface. It should be noted that the 2.5-layer values agree well with those obtained by Lauter *et al.* who report a single measurement made at about the same coverage.[6]

Although our independent-layer model fits the data, it cannot be said to represent a definitive determination of the structure. Normally, this would require confirming evidence from higher-index diffraction peaks. As it happens, the large Debye-Waller factors of helium films make it unlikely that additional Bragg peaks will be detectable at scattering angles

larger than those investigated here. Thus we must also ask if there are other equally valid interpretations of the data. One possibility that comes to mind is that the film undergoes a transition from a triangular-lattice monolayer to an oblique bilayer such as, for example, that characterized by the unit cell shown in Fig. 2(b) which has sides of length 3.57 and 3.15 Å and an included angle $\alpha = 60°$. This cell has d spacings consistent with the positions of the two Bragg peaks observed in the higher-coverage scans. Moreover, the nearest- and next-nearest-neighbor distances are exactly the first- and second-layer nearest-neighbor distances in our earlier considered independent-layer model while the layer density—0.103 atoms/Å^2—is intermediate between the densities of the first and second layers in the previous model. In fact, two layers having the density of the cell of Fig. 2(b) would contain the same number of atoms as the independent bilayer of Fig. 2(a).

A little reflection shows that any oblique cell with d spacings of length 3.09 and 2.72 Å will produce a diffraction profile like that observed; values of $\alpha < 60°$ simply give a cell of larger area while values of $\alpha > 60°$ have the opposite effect. We chose the cell of Fig. 2(b) because it leads to bilayer completion at a coverage consistent with specific heat and vapor pressure isotherm measurements.

To estimate the relative intensity of the Bragg reflections from an oblique layer, it is necessary to assume a specific packing arrangement for the second layer. A calculation of the structure factor with the second-layer atoms located at the positions shown in Fig. 2(b) leads to a prediction that the ratio of intensities of the two Bragg peaks at $2\theta = 47°$ and 54° should be 0.45. This is somewhat below the observed range of 0.55 to 0.64 noted above. However, introducing a Debye-Waller factor for the bilayer would tend to bring the calculated intensity ratio closer to that observed experimentally.

Viewed in terms of the criteria thus far considered, the two structures are experimentally indistinguishable. Nevertheless, there is one difference between the low-index diffraction patterns of the independent and oblique bilayer structures which ought to make it possible to choose between them; the latter, in addition to peaks at $2\theta = 48°$ and 53°, should also have a peak at 51° with an intensity about 0.84 of that of the 48° peak. In principle, the presence or absence of this peak should establish which is the correct structure. Unfortunately, helium is a very weak neutron scatterer and the statistical uncertainties in the data make it difficult to say conclusively if there is or is not a diffraction peak in the angular range of interest.

Since second-layer ordering is clearly the result of a delicate balance between He-C and He-He interactions, it might be relevant to note at this point that the ratio of the d spacing of the (10) reflection from the oblique bilayer ($d = 3.09$ Å) to the graphite basal-plane lattice constant ($a = 2.46$ Å) is almost exactly 5:4. This suggests that the oblique bilayer might be stabilized by the graphite substrate. For the independent bilayer, the equivalent quantity—the ratio of the lattice constant of the highly compressed underlayer ($a = 3.15$ Å) to that of the graphite basal plane—is less favorable; it deviates by more than 2% from 5:4; thus the stabilizing effect of the substrate would be less pronounced. On the other hand, we think it not unlikely that the substrate interaction could produce the same kind of density gradient in the solid that it does in the liquid. This effect would work in the opposite direction, favoring the independent bilayer over its oblique counterpart.

Finally, completeness requires that we mention another possible interpretation of the diffraction patterns observed above monolayer coverage; this is that the second layer does not solidify at all, the low-angle peak which appears being, in this view, one of a pair of symmetrically positioned satellites produced by either periodic strains or a periodic domain-wall structure in the first layer. Indeed, the trailing edge of the first peak does show some slight evidence of structure, possibly significant, in the region expected. If strains occur, however, it is difficult to understand why they appear only at higher coverages. Thus we think this a less likely explanation although we cannot rule it out altogether.

B. Overlayer enhancement of the graphite (002) reflection

Even when incommensurate, surface films can contribute coherently to the scattering from graphite (00l) planes,[11] altering the intensities of the graphite peaks and, when the height of the film above the surface is not the same as the spacing between the substrate basal planes, shifting their positions as well. Plotted in Fig. 3 are difference scans made in the neighborhood of the graphite (002) reflection, the scattering coming, in this case, from 90° misoriented graphite crystallites. There is evidence of small changes in the scattered intensity and, more importantly, of slight shifts in peak position due to the presence of the helium film. On a substrate of N atomic layers, the difference between diffracted intensities with and without a surface overlayer is given by a relation of the form[12]

$$I_{s+a}(Q_z) - I_s(Q_z) = b_a^2 + 2b_a b_s \{\cos[\tfrac{1}{2}(N+1)Q_z d + Q_z \delta]\} \left(\frac{\sin N Q_z d/2}{\sin Q_z d/2} \right) , \quad (1)$$

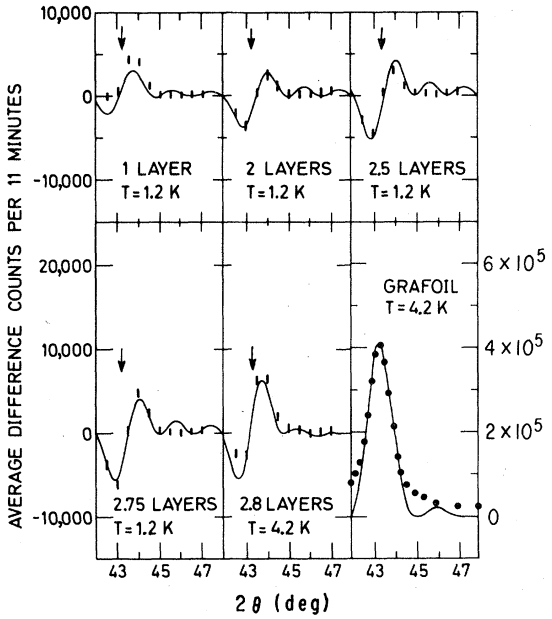

FIG. 3. Coverage dependence of difference-diffraction profiles from ^{4}He films on Grafoil obtained in the neighborhood of the graphite (002) peak. The arrow shows the position of the graphite (002) peak observed with no helium in the cell; the solid lines are fits to the data using a modified form of Eq. (1) which takes account of contributions from the second (and third) atomic layers. Details are given in the text.

where the subscripts s and a refer to the substrate and adsorbed layer, respectively, d is the distance between substrate planes, $d+\delta \equiv \langle z \rangle$ is the height of the adsorbed layer above the surface, b_s and b_a are the relevant scattering amplitudes per unit area, and Q_z is the projection of the scattering vector $\vec{Q}$ on the c-axis direction of the substrate crystallite. The above expression shows that the observed shift in the peak position is directly related to the location of the helium film above the graphite basal plane: A measurement of the (002) shift is thus a way of determining the film height.

Although simple in concept, the method is not without experimental complications. Of these, the most serious is that systematic errors in the positioning of the spectrometer arm can substantially reduce the sensitivity of the measurement or even make it impractical altogether. Long-term annealing of the film or extinction effects due to the introduction of a strongly scattering adsorbed layer can also cause difficulties. We remarked earlier that care was taken to be certain that the scans were reproducible within statistics. Noting further that helium is not a strong scatterer of neutrons and should not significantly alter the extinction characteristics of the sample, we believe the difference profiles of Fig. 3 genuinely to arise from interference between film and substrate scattering.

To extract an accurate value of the film height from the experimental data requires averaging Eq. (1) over the size distribution of substrate crystallites and then folding the result with the resolution function of the spectrometer. We determined the crystallite size distribution or, to be more precise, the distribution of N (the number of basal plane layers per crystallite), to sufficient accuracy for our purposes by assuming N to have a Gaussian functional form $(\exp\{-\frac{1}{2}[(N-N_0)/\Delta N)]^2\})$, calculating the line shape for such a distribution and fitting the result to the experimentally observed profile of the (002) reflection from our Grafoil substrate. Best fit was obtained with $N_0=31$ and $\Delta N=6$. Equation (1), when weighted with this distribution and folded with the instrument resolution, yielded curves which were reasonable representations of the observed difference profiles. (In making the calculations, we assumed that films on both the top and bottom surfaces of each crystallite contributed to the scattering.) The solid line in Fig. 4 shows the best fit to the monolayer data of Fig. 3; it yielded $\langle z_1 \rangle = 2.85$ Å for the height of the film above the graphite surface. An equivalent calculation, made with the same value of $\langle z_1 \rangle$ but with $N_0=28$ and $\Delta N=0$, gave the result plotted as the dashed line in the figure. Note that it is not substantially different, indicating that the analysis is not overly sensitive to either the value of

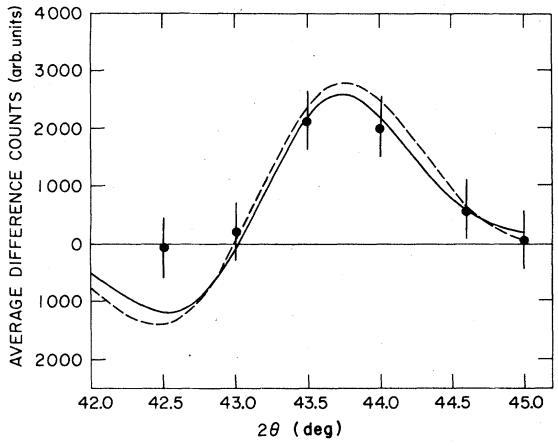

FIG. 4. Difference-diffraction profiles calculated from Eq. (1), assuming (i) a Gaussian distribution of N (the numer of basal plane layers per crystallite) of the form $\exp\{-\frac{1}{2}[(N-N_0)/\Delta N]^2\}$, and (ii) that both the top and bottom surfaces of each crystallite are covered with a single layer of ^{4}He atoms. The curves were calculated with the height of the film above the graphite plane fixed at the best-fitting value, 2.85 Å. Solid line: $N_0=31$, $\Delta N=6$. Dashed line: $N_0=28$, $\Delta N=0$. Solid circles: experimental data.

N_0 or ΔN used in the computation. It should also be noted that both calculations predict an initial negative swing in the difference profile which is not observed experimentally. We have not been able to track down the reason (or reasons) for this discrepancy.

Applying Eq. (1) to the higher-coverage data of Fig. 3 requires that it be modified to take account of second- and third-layer contributions. We found when we did this that it led us into difficulties. The measurements were not sensitive enough to obtain unique values for more than a single-layer spacing. To make the least-squares-fitting routine converge, it was therefore necessary to fix the first-layer spacing before the second could be determined and, correspondingly, to fix the first- and second-layer spacings to determine the third. Vertical compression of the layers almost certainly occurs and makes the procedure somewhat arbitrary. Being uncertain of its reliability, we simply note as a matter of record that at 1.2 K the best fit was obtained with $\langle z_2 \rangle = 2.40$ Å and $\langle z_3 \rangle = 3.8$ Å. At 4.2 K, the equivalent values found were $\langle z_2 \rangle = 2.8$ Å and $\langle z_3 \rangle = 4.0$ Å. In each case $\langle z_1 \rangle$ was held fixed at 2.75 Å.

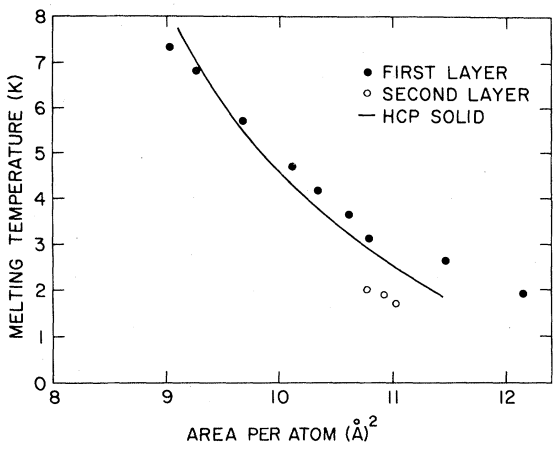

FIG. 5. Dependence of the melting temperature on the atomic area $(1/\rho)$ assuming independent solid layers. Solid circles: first layer (Ref. 10). Open circles: second layer (area per atom measured at 1.2 K). Solid line: bulk hcp helium (Ref. 13). For the hcp solid, the atomic areas are those in the basal plane. Thermal expansion will shift the second-layer points to the right. Whether the first- and second-layer data would then fall on a single, universal curve is an open question.

IV. DISCUSSION

As we have shown, the diffraction patterns of helium films adsorbed on graphite at coverages above two layers and at temperatures below 1.2 K are consistent with either of the two structural models of Fig. 2: (i) a solid composed of two incommensurate triangular layers [Fig. 2(a)]; or (ii) an ordered oblique bilayer [Fig. 2(b)]. Unfortunately, the limits imposed by the statistical accuracy of the present data make it difficult to decide which is the correct choice although this might be possible in the future if data with less statistical uncertainty can be obtained.

It is an interesting and surprising fact that helium monolayers adsorbed on graphite melt at about the same temperature as hcp solid helium with the same basal-plane atomic density. Plotted in Fig. 5 are melting temperatures for the three-dimensional hcp solid phase at various basal-plane densities[13] (solid line) and for the first adsorbed helium layer[10] (solid circles). By combining the results of heat-capacity measurements with our neutron-diffraction data, we can make a similar plot for the second layer. Assuming the peak observed in the specific heat represents the melting of an incommensurate second solid layer [i.e., assuming the structure of Fig. 2(a) to be the correct one], we can use the specific-heat measurements of Ref. 4 to define the melting temperature and the data of Table I to define the second-layer density. These points—plotted as the open circles in Fig. 4—lie below the bulk melting curve, suggesting that the second layer—if it is an independent layer—expands significantly between 1.2 K and the melting temperature.

Both our measurements and the heat-capacity studies of Ref. 4 show that there is a critical density below which helium atoms in the second layer do not solidify. Assuming as before an independent-layer structure, we estimate from the data of Table I that the limiting value is 0.091 atoms/Å^2 compared to an equivalent value of 0.086 atoms/Å^2 for the basal plane of the hcp solid phase at the same temperature.[14]

Finally, it is of interest to ask what has been learned about the He-C interaction from our measurement of the height of the helium monolayer above the graphite basal plane. Carlos and Cole[15] have analyzed heilum-graphite gas scattering experiments using a number of different functional forms to represent the He-C pair potential. Their conclusion was that sums of anisotropic Yukawa-6 or Lennard-Jones 6-12 pairwise interactions best fitted both the observed bound-state energies and the matrix elements, the Lennard-Jones form appearing to be slightly the better choice, although the evidence in its favor was not conclusive. Cole and Toigo have since used both functional forms to calculate helium-atom probability densities to obtain values for $\langle z_1 \rangle$, the most probable position of the helium monolayer above the graphite surface.[16] They find $\langle z_1 \rangle = 2.45$ and 2.89 Å for the Yukawa and Lennard-Jones forms, respectively. Our value, $\langle z_1 \rangle = 2.85$ Å, clearly favors the latter.

ACKNOWLEDGMENTS

We would like to express our appreciation to Dr. M. W. Cole for a number of helpful discussions and for communicating the results of his calculations to us in advance of publication. We also thank R. Wang for assistance with the computer calculations. K.C. wishes to thank Brookhaven National Laboratory for hospitality extended to him. He also wishes to thank NATO for financial assistance. Work at Brookhaven was supported by the Division of Basic Energy Sciences, U.S. Department of Energy, under Contract No. DE-AC02-76CH00016. Work at the University of Missouri-Columbia was supported by the National Science Foundation under Grant No. DMR-7905958.

---

[1]Grafoil is the trademark of an expanded graphite product marketed by the Union Carbide Corporation, Carbon Products Division, 270 Park Avenue, New York, New York 10017.

[2]M. Bretz, J. G. Dash, D. C. Hickernell, E. O. McLean, and O. E. Vilches, Phys. Rev. A 8, 1589 (1973).

[3]K. Carneiro, W. D. Ellenson, L. Passell, J. P. McTague, and H. Taub, Phys. Rev. Lett. 37, 1695 (1976).

[4]M. Bretz, Phys. Rev. Lett. 31, 1447 (1973).

[5]S. E. Polanco, J. H. Quateman, and M. Bretz, J. Phys. (Paris) 39, C6-344 (1978).

[6]H. Lauter, H. Wiechert, and R. Feile, in *Proceedings of an International Conference, Lake Geneva, Wisconsin, 1980,* edited by S. K. Sinha (Elsevier North-Holland, New York, 1980), p. 291.

[7]The layer densities quoted were obtained by combining results from Refs. 2 and 5 which reported, respectively, heat-capacity studies of helium films on Grafoil and on exfoliated *ZYX* graphite. A smaller value of the second-layer density (0.079 atoms/Å^2) was obtained from an earlier (and presumably less reliable) measurement made on Grafoil and reported in Ref. 4.

[8]Warren's formula is used in the analytic form given by J. K. Kjems, L. Passell, H. Taub, and A. D. Novaco, Phys. Rev. B 13, 1446 (1976). References to Warren's original derivation of the formula can be found in that paper.

[9]W. Marshall and S. W. Lovesey, *Theory of Thermal Neutron Scattering* (Oxford University Press, London, 1971), derive the three-dimensional form of this expression.

[10]M. Bretz, G. B. Huff, and J. G. Dash, Phys. Rev. Lett. 28, 729 (1972).

[11]C. Marti, B. Croset, P. Thorel, and J. P. Coulomb, Surf. Sci. 65, 532 (1977).

[12]H. Taub, K. Carneiro, J. K. Kjems, L. Passell, and J. P. McTague, Phys. Rev. B 16, 4551 (1977).

[13]G. Ahlers, Phys. Rev. A 2, 1505 (1970).

[14]C. A. Swenson, Phys. Rev. 79, 626 (1950).

[15]W. E. Carlos and M. W. Cole, Surf. Sci. 91, 339 (1980).

[16]M. W. Cole and F. Toigo, Phys. Rev. B 23, 3914 (1981).